ISSN 1392 - 1207. MECHANIKA. 2005. Nr.6(56)

Creation and investigation of membrane actuator for nanopositioning using laser micro-machining

V. Lendraitis*, V. Snitka, R. Barauskas*****

**Kaunas University of Technology, Studentų 65, 51369 Kaunas, Lithuania, E-mail: vitas.lendraitis@ktu.lt*
***Kaunas University of Technology, Studentų 65, 51369 Kaunas, Lithuania, E-mail: vsnitka@ktu.lt*
****Kaunas University of Technology, Studentų 50, 51368 Kaunas, Lithuania, E-mail: rimantas.barauskas@ktu.lt*

1. Introduction

Significant advances in smart material actuators have taken place in the past years. The holy grail of actuator research is an architecture that can generate high displacement and force throughout a broad frequency range while not consuming a significant amount of electrical power.

Many micro/nanorobotic application require multi degree of freedom positioning at micro and nanoscales. Actuation technologies capable of providing motion at this scale includes piezoactuators [1], microstepping motors, highly geared electromagnetic servomotors and Lorentz force-type actuators such as voice coil motors [2]. The nanotechnology applications require more complex specifications, including the wide dynamic range of nanopositioning systems. It means the new, innovative solutions have to be found for the actuation methods, materials, and design. The silicon as mechanical material and laser micromachining opens a new possibilities in actuator design.

Microfabrication with lasers today is in such a situation when struggle takes place in two fronts: machining quality and efficiency. Quasi-cw and Q-switched lasers act as a pure thermal heat source. Those, nanosecond, lasers are time effective tools, but they require additional steps to remove recast. One of the promising ways for the progress in laser machining is the use of shorter pulses. They enable to decrease the remaining thermal impact and ablation threshold [3, 4]. On the other hand, ultra-short pulses come at the expense of added complexity. Moreover, a femtosecond beam on its way from a laser source to a workplace experiences spatial distortion in the air by cold plasma [5]. It was found that femtosecond pulses alone are not sufficient to produce recast-free structures in metals. Melt-free material processing is only possible in a restricted parameter window [6]. Normally, certain optimal pulse duration exists for machining, at least in materials that can directly absorb the laser beam - metals and semiconductors. Both are in picosecond timescale: for steel it is about 10 ps [4] and for silicon it is below 5 ps [4].

Interest in picosecond lasers has increased recently. They have the potential to improve machining quality as compared to that achievable with longer pulses [6]. As femtosecond systems are complicated and the advantages of processing with ultra-short pulses are evident only at low laser fluences, picosecond lasers present a cost-effective alternative for machining of micro objects. Real industrial applications of ps-pulses require reliable laser sources and well established technologies. In this work we present the theoretical modeling and experimental results of our research on microfabrication of silicon actuator by picosecond laser.

2. Electrostatic model of actuator

To model the working of electrostatic actuator is to consider a rigid plate attached by a spring placed in an electrostatic field (Fig. 1).

For the simulation of the system represented in Fig. 1, the calculation is based on the mechanical law governing the electrostatic actuator which can be expressed as follows

$$m\frac{d^2W}{dt^2}+\lambda\frac{dW}{dt}+KW=\frac{\varepsilon U^2}{2\left(e-W\right)^2}A^2 \qquad (1)$$

where W is the deflection; m is the mass; λ is the damping factor; K is the spring value. K depends on the geometry of the microstructure. The excitation is represented with the electrostatic pressure through a gap applied on the plate surface S, with the voltage U and the permittivity e. The mass can be expressed with the geometrical characteristics of the plate $m = \rho hA$, here ρ is material density; h is plate thickness; A is area of plate surface.

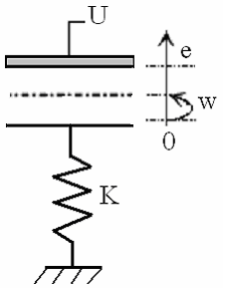

Fig. 1 Simple model of an electrostatic actuator

The material properties of the membrane actuator are listed in Table 1.

Table 1

Material characteristics of membrane actuator

Materials	E, GPa	v	ρ, 10^3 kg/m^3	h, μm
Al	70.3	0.345	2.69	0.3
Si (substrate)	120	0.42	2.33	300

Note: E is Young module; v is Poison coefficient; ρ is material density; h is plate thickness.

Using the finite element method, the construction investigation is performed, where the structure is meshed by simple geometry finite elements and the type of them depends on the task solved. The ANSYS software package was selected for the analysis of membrane actuator. Shell 43 type finite elements were chosen to model this type of structures. These elements are usually used to model plane structures of various thickness and elastic material constructions (Figs. 2 and 3). Shell43 is a 4-nodes plastic large strain element [7].

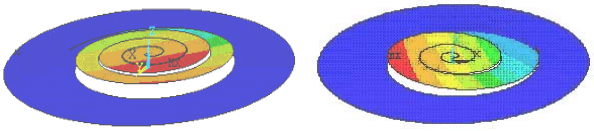

a b

Fig. 2 Actuator displacement in static mode: a - Archimedes curve spring, displacement out of plane - 49 µm; b - conical spring, displacement out of plane - 16 µm. Gap between plate -140 µm, control voltage -200V

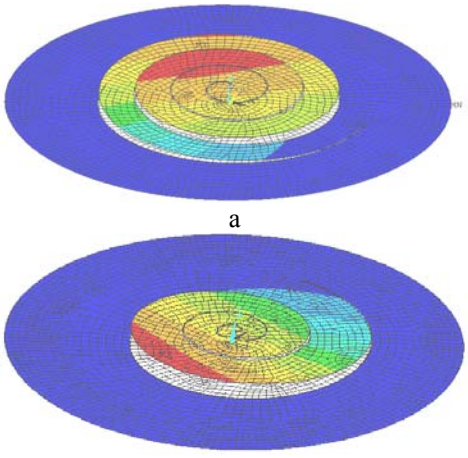

a

b

Fig. 3 Actuator displacement in dynamic mode: a- for Archimedes curve spring the frequency *f*=132 Hz; b- conical spring the frequency *f*= 253 Hz

Figs. 4 - 7 show the results of a driving micro actuator at 0-200 V applied voltage.

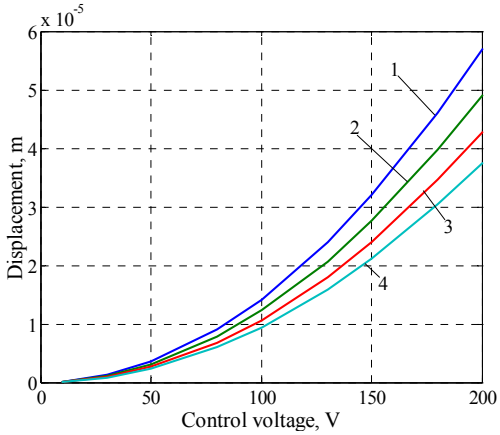

Fig. 4 Four turns Archimedes curve spring: *1*- a gap between the plates -130 µm; *2*-a gap between the plates - 140 µm; *3* - a gap between the plates - 150 µm; *4*- a gap between the plates- 160 µm

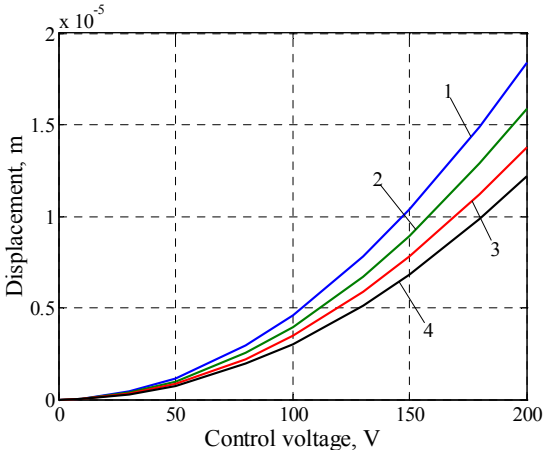

Fig. 5 Four turns conical spring: *1* - a gap between the plates - 130 µm; *2* - a gap between the plates - 140 µm; *3* - a gap between the plates - 150 µm; *4* - a gap between the plates - 160 µm

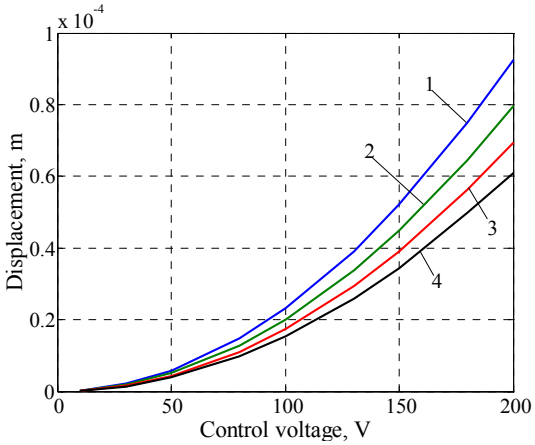

Fig. 6 Five turns Archimedes spring: *1* - a gap between the plates - 130 µm; *2* - a gap between the plates - 140 µm; *3* - a gap between the plates - 150 µm; *4* - a gap between the plates - 160 µm

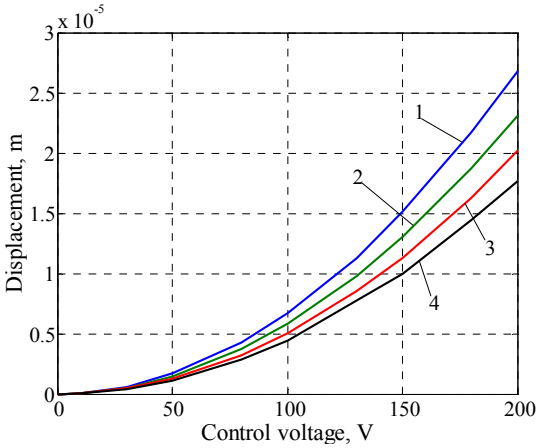

Fig. 7 Five turns conical spring: *1* - a gap between the plates - 130 µm; *2* - a gap between the plates - 140 µm; *3* - a gap between the plates - 150 µm; *4* - a gap between the plates - 160 µm

3. Experimental set-up

Laser machining experiments were performed on the workstation that included picosecond laser, beam de-

livery system and galvanoscanner. The laser with a regenerative amplifier (PL2241, EKSPLA Ltd.) generated pulses of 60 ps duration at 1064 nm wavelength and 250 Hz repetition rate (Figs. 8 and 9). Attenuator made of a half-wave plate and polarizer was used to change laser pulse energy. Scanner ScanGine14 (Scanlab) with the f-theta lens of the 160 mm focal length was used for the laser beam stearing. The spot diameter was 35-30 μm.

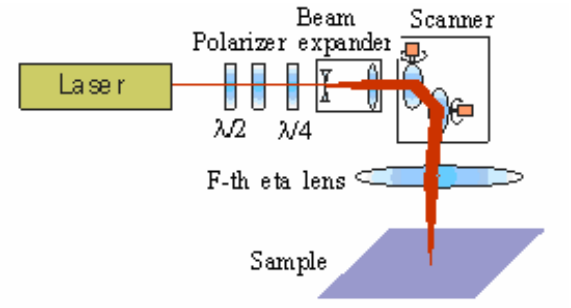

Fig. 8 Scheme of experimental set-up

Experiments were performed on silicon wafers with thicknesses 300 μm. The pulse energy, overlap and number of scans were varied during cutting experiments.

Fig. 9 Experimental setup for AFM investigations

4. Micromachining

The design goals are as follows: Stroke, Output force, Driving voltage. The stroke in the out-of-plane direction needs to be 40 μm. The driving voltage needs to be less than 250 V. Design of actuator geometries using laser micro- machining are shown in Fig. 10.

The range for "gentle" machining of silicon with ps-laser was estimated in previous experiments [8]. The increase in the ablation rate at fluences >100 J/cm^2 was accompanied by crack formation around the upper rim of the hole. All the experiments in this work were performed with ps-laser fluence well below this value. Recast material was spread within the distance of 42 μm with burr height of 0.3 μm (Fig. 11). It can be easily removed by soak into an ultrasound bath for 10 min. According to the investigations made in silicon at high laser fluences, a recast layer on walls does not disappear even for 200 fs pulses [5]. Heat from the recast material stimulates the formation of a heat-affected zone (HAZ) irrespective of applied pulse duration.

The number of laser pulses required for throughout drilling depends on laser fluence and wafer thickness. Fig. 12 represents the results obtained in wafers of various thicknesses. At least 100 pulses need to be applied at high fluence, when for lower pulse energy the number increases

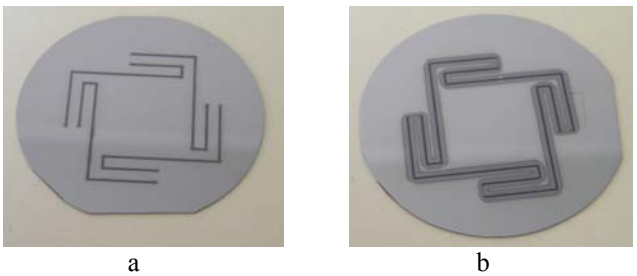

Fig. 10 Design comparison of actuator geometries using laser micro - machining: a - plane flexures; b - plane flexures 50 μm deepening; c - Archimedes curve spring; d - conical spring

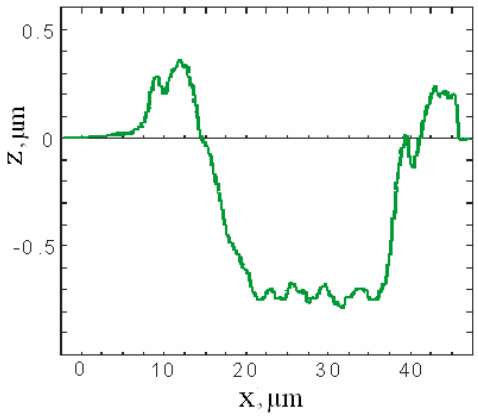

Fig. 11 Profile of a single-shot crater in silicon (12 J/cm^2, 266 nm)

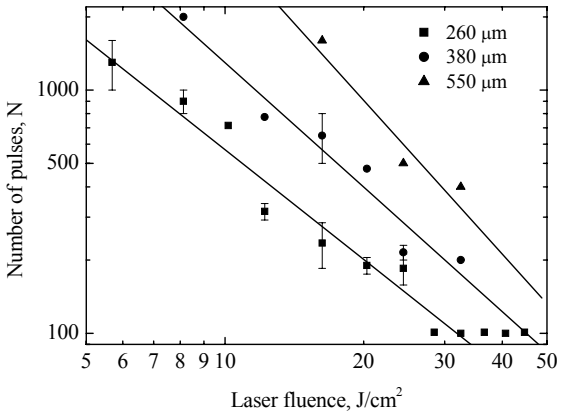

Fig. 12 Percussion drilling rate in silicon Lines - fitting $N \sim F^Y$ (y= 1.5, 1.7, 2.1 for wafer thickness of 260, 380 and 550 μm)

rapidly. The solid line shows the $\boldsymbol{N \sim F^{-1.5}}$ relationship between laser fluence and the number of pulses, which quite well describes the results below 30 J/cm^2 in the 260 μm-thick wafer. For wafers of 380 μm and 550 μm thick, the power increases to 1.7 and 2.1 correspondingly. This more rapid increase in the number of pulses for

through-out drilling in thicker samples reflects the shielding action of plasma inside a hole [4]. The limit for throughout drilling exists at low fluence side. For 260 µm wafer it is below 6 J/cm^2.

Scribing and cutting of silicon wafer were performed using different pulse overlap and various numbers of consecutive scans. Laser fluence was chosen from the region of "gentle" ablation, below 50 J/cm^2. Attained cutting speed was very low because of the low repetition rate of the laser. The kerf width was 35-40 µm wide, which was bigger than the spot size (25 µm) (Fig. 13). The rim of the kerf on the entry side was always sharp, smooth and crack-free.

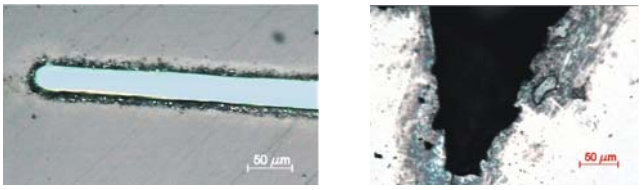

Fig. 13 Comparison of cuts made in silicon by 60 ps @ 266 nm (left) and 15 ns @ 355 nm (right) laper pulses

5. Results

Actuators displacement was investigated by atomic force microscope (AFM) Quesant QScope-250 in contact mode with cantilever force constant 0.1 N/m. The displacement was measured applying direct current voltage to the actuator and imaging the actuator surface during the scan. The surface 3D image is presented in Fig. 14. The displacement was measured directly from the AFM image cross-section.

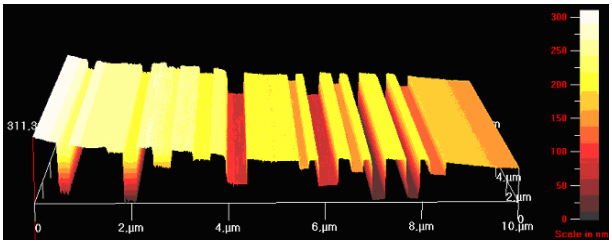

Fig. 14 Actuators surface displacement AFM image in static mode at different control voltage

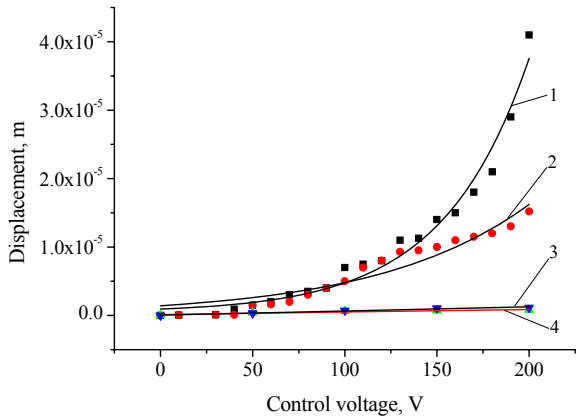

Fig. 15 Static experimental results. Displacement from the natural position: *1* - Archimedes curve spring; *2* - conical spring; *3* - plane flexures 50 µm deepening; *4* - plane flexures

The driving characteristics of the Archimedes curve spring, conical spring, plane flexures 50 µm deepening and flexures were also examined. Fig. 15. shows the characteristics of the tip height versus the applied voltage. Driving voltage was used 0-200 V. The gap between the plates is 140 µm.

The experimental investigation demonstrated good agreement between computer simulation results (Figs. 4 - 7) and experiment results (Fig. 15).

It was demonstrated that silicon micro machined electrostatic driven actuators can be used in different nanomanipulating systems.

Further research includes the realization of actuators for Scanning Probe Microscopy applications.

6. Conclusions

1. The work of membrane actuator in the static and dynamic mode was modeled applying the Finite elements method.

2. The experiment investigation have been made on silicon membranes fabricated by laser micro- machining. Investigation of pico and femtosecond laser cutting technique, demonstrate that femtosecond laser cutting produce less distorted cutting line and less damaged material.

3. Static and dynamic characteristics were investigated. It was demonstrated that the developed actuator produces the 40 micron displacement under the 200 V control voltage. The determined first mode resonance frequency was 132 Hz – for Archimedes curve spring, 252 Hz- for conical spring, 365 Hz- plane flexures 50 µm deepening and 400 Hz- for plane flexures.

4. Applying AFM system, the static characteristics of membrane actuator were evaluated.

5. The positive investigation results of membrane actuator allow optimizing the membrane construction and designing the scanning microscopy nanopositioning devices.

References

1. **Szita, N., Sutter, R., Dual, J. and Buser, R.A.** A micropipettor with integreted sensors.-Sensors and Actuators A, 2001, v.89, No1-2, p.112-118.
2. **Molenaar, A., Zaaijer, E. H. and van Beek, H.F.** A novel long stroke planar magnetic bearing actuator.-Proc. of the 4th Int. Conf. on Motion and Vibration Control, 1998, p.1071-1076.
3. **Nolte, S., Momma, C., Jacobs, H., Tunnermann, A., Chichkov, B.N., Wellegehausen, B. and Welling, H.** Ablation of metals by ultrashort laser pulses. -J. Opt. Soc. Am. B., 1997, p.2716-2722.
4. **Liu, X., Du, D., & Mourou, G.** Laser ablation and micromachining with ultrashort laser pulses.-IEEE J. Quantum Electronics, 1997, 33, 10, p.1706-1716.
5. **Dausinger, F.** Machining of metals with ultrashort laser pulses: fundamental aspects and their consequences.-CLEO/Europe, Munich, Germany, June 23-27, 2003, p.491-498.
6. **Weikert, M., Foehl, Ch., Dausinger F.** Surface structuring of metals with ultrashort laser pulses.-Proc. 3d Int. Symp. on Laser Precision Microfabrication, Proc. SPIE 2003, p.501-505.

7. ANSYS, Revision 8.0, Swanson Analysis Systems Inc. - Houston, USA, 2003.-568p.
8. **Luft, A., Franz, U., Emsermann, A. & Kaspar, J.** A study of thermal and mechanical effects on materials induced by pulsed laser drilling.-Appl. Phys.A, 63, p.93-101.

V. Lendraitis, V. Snitka, R. Barauskas

MEMBRANINIO AKTIUATORIAUS NANOPOZICIONAVIMUI KŪRIMAS IR TYRIMAS NAUDOJANT LAZERINĮ MIKROAPDIRBIMĄ

R e z i u m ė

Straipsnyje nagrinėjama galimybė panaudoti Si membranas mikroobjektams nanopozicionuoti.

Baigtinių elementų metodu nustatytos membraninio mikroaktiuatoriaus pagrindinės rezonansinės modos ir jų priklausomybė nuo skirtingos geometrijos Si plokštelių. Taikant mikrosistemų konstravimo technologijas sukurtas membraninio mikroaktiuatoriaus prototipas. Naudojant atominių jėgų mikroskopo sistemą, nustatytos membraninių struktūrų statinės ir dinaminės charakteristikos.

Tyrimo rezultatai naudotini kuriant naujo tipo skenuojančios mikroskopijos nanopozicionavimo sistemas.

V. Lendraitis, V. Snitka, R. Barauskas

CREATION AND INVESTIGATION OF MEMBRANE ACTUATOR FOR NANOPOSITIONING USING LASER MICRO-MACHINING

S u m m a r y

The article deals with the possibility to apply Si membranes for nanopositioning of microobjects.

Applying the finite element method the basic resonant modes and their dependence on different geometry Si plates are identified. The prototype of membrane micro actuator was designed applying microsystem designing technologies. Using the atomic force microscopy system, static and dynamic characteristics of the membrane structures were defined.

The results of the investigation could be applied in developing a new type of nanopositioning systems of scanning microscopy.

В. Лендрайтис, В. Снитка, Р. Бараускас

ИСПОЛЬЗОВАНИЕ ЛАЗЕРНОЙ МИКРО ОБРАБОТКИ ПРИ СОЗДАНИИ И ИССЛЕДОВАНИИ МЕМБРАННОГО АКТЮАТОРА ДЛЯ НАНОПОЗИЦИОНИРОВАНИЯ

Р е з ю м е

В статье рассматривается возможность использования мембран из кремния (Si) для позиционирования микрообъектов с нанометрической точностью.

Методом конечных элементов определены основные резонансные моды мембраны и их зависимость от различной геометрии пластинок. Используя технологии конструирования микросистем создан прототип мембранного микроактюатора. При помощи системы микроскопа атомных сил определены статические и динамические характеристики созданных мембранных структур.

Результаты исследования могут быть использованы при создании нанопозиционирующих устройств нового типа для сканирующей микроскопии.

Received May 19, 2005